Artesunate combined with verteporfin inhibits uveal melanoma by regulation of the *MALAT1*/yes-associated protein signaling pathway

XUDONG JIU[1], YANG LIU[1] and JIN WEN[2]

[1]Department of Ophthalmology, The First Hospital of Lanzhou University, Lanzhou, Gansu 730020; [2]Department of Ophthalmology, People's Hospital of Gansu Province, Lanzhou, Gansu 730000, P.R. China

Received February 4, 2021; Accepted May 12, 2021

DOI: 10.3892/ol.2021.12858

Abstract. Uveal melanoma (UM) is the most common ocular malignancy and has no effective clinical treatment. Therefore, novel drugs to suppress UM tumor progression are urgently required. The present study aimed to clarify the underlying mechanism of the inhibitory effects of artesunate on UM. By using plasmid transfection and detecting apoptotic level, the present study identified artesunate as a potential candidate for UM treatment. Compared with those in the vehicle (DMSO)-treated control cells, artesunate enhanced the apoptotic rate and increased lactate dehydrogenase release, reactive oxygen species and IL1b and IL18 levels in C918 cells. Overexpression of yes-associated protein (YAP) or metastasis-associated lung adenocarcinoma transcript 1 (*MALAT1*) in C918 cells reversed the effects of artesunate and reduced the apoptotic rate compared with those observed in cells transfected with the negative control plasmid. Notably, verteporfin enhanced the effects of artesunate on C918 cells by increasing the apoptotic rate, indicating that combined therapy was more effective compared with treatment with artesunate alone. In conclusion, the results of the present study demonstrated that artesunate elevated the apoptotic rate and suppressed C918 cell viability by regulating the *MALAT1*/YAP signaling pathway, and these effects were enhanced by supplementation with verteporfin. These results suggested that artesunate may exert an inhibitory effect on C918 cells and that the *MALAT1*/YAP signaling may serve important role in mediating these effects, providing evidence of its potential for treating UM in the clinic.

Correspondence to: Professor Jin Wen, Department of Ophthalmology, People's Hospital of Gansu Province, 204 Donggangxi Road, Lanzhou, Gansu 730000, P.R. China
E-mail: 67859694@qq.com

Key words: artesunate, uveal melanoma, apoptosis, *MALAT1*, yes-associated protein, combination therapy

Introduction

As a common primary tumor in adults, uveal melanoma (UM) accounts for 3.7% of all melanomas (1). Numerous risk factors are associated with UM, including age, sex, genetic or phenotypic predisposition, work environment and dermatological conditions (2). UM has a strong propensity for fatal metastasis (3) and frequently metastasizes to the liver via the hematogenous route; according to data from 2005, 90% of UM metastases occur in the liver (4), which results in a dismal prognosis (5). Additionally, severe inflammation has been identified in UM cells (6,7), particularly those with mutations of G protein subunit α (GNA)11 or GNAQ, which trigger a wide range of cell signaling cascades, including the PI3K/Akt/mTOR and YAP/TAZ pathways (2); however, limited approaches are available to alleviate inflammation in UM, as the eye is an immunologically privileged site, which provides UM with a protective niche (8). To date, several strategies have been adopted to treat UM in the clinic, including surgical resection, immunotherapy (9) and gamma knife radiosurgery (10). For example, ipilimumab, an anti-cytotoxic T-lymphocyte-associated protein 4 antibody, elicits a positive response in 40-60% of patients with metastatic cutaneous melanoma (2), providing a potential new treatment for UM in the clinic. Recently, small molecules, such as selumetinib (11), nivolumab (12), ipilimumab (12) and selumetinib in combination with dacarbazine (13), have been identified as potential inhibitors of tumor progression able to improve the prognosis of patients with UM, although the underlying mechanisms remain elusive. Overall, there is a need to identify novel drugs for UM treatment and explore their underlying mechanisms.

Artemisinin is a natural product derived from the Chinese herb *Artemisia annua* (14). As a stable derivative of artemisinin, artesunate exhibits robust antimalarial activity in mammals (15,16), as well as various physiological activities, including inhibiting inflammation (17) and nervous system protection (18). For example, Zeng *et al* (17) have reported that artesunate inhibits the Toll-like receptor 4/tumor necrosis factor receptor-associated factor 6 and phosphoinositide-specific phospholipase C1/Ca^{2+}/nuclear factor of activated T cells 1 signaling pathways and

improves lipopolysaccharide-induced osteoclastogenesis in RAW264.7 cells and mice. Another study used electrophysiological assays and histopathological examination to demonstrate that topical artesunate treatment has a positive effect on peripheral nerve regeneration (18). In addition, artesunate exhibits antitumor effects against several types of cancer cells, including lymphoma (19,20), head and neck cancer (21) and hepatocellular carcinoma (22), and suppresses the MEK/ERK and PI3K/Akt signaling pathways in HL-60 cells, inducing apoptosis and inhibiting leukemia cell proliferation (23). Additionally, artesunate induces apoptosis by activating reactive oxygen species (ROS)- and p38 MAPK-mediated signaling and suppresses embryonal rhabdomyosarcoma cell proliferation (24); however, a limited number of studies have focused on the effect of artesunate on UM progression (25,26).

Apoptosis is a form of programmed cell death that occurs in multicellular organisms and is characterized by various cellular changes, ranging from nuclear fragmentation to global mRNA decay (27). In mammals, apoptosis exerts positive effects on cell self-renewal (28). In addition, apoptosis serves critical roles in tumor growth, including colon cancer (29,30), pancreatic ductal adenocarcinoma (31) and acute myeloid leukemia (32). For example, Nangia *et al* (33) have demonstrated that treatment with a combination of MEK and myeloid cell leukemia-1 (MCL1) inhibitors induces apoptosis by regulating MCL1, leading to inhibition of cell proliferation in a KRAS-mutant non-small cell lung cancer model. In addition, the proliferation of hepatocellular carcinoma cells is suppressed by elevating the levels of apoptosis following CBX2 knockdown (34). Notably, artesunate exerts antitumor activity by enhancing apoptosis; Zhou *et al* (35) have reported that artesunate upregulates ROS levels and activates the AMP-activated protein kinase/mTOR/unc-51-like autophagy-activating kinase 1 axis in T24 cells, resulting in autophagy-dependent apoptosis of human bladder cancer. However, whether artesunate treatment enhances UM cell apoptosis and the potential underlying mechanisms of this effect are poorly understood. The metastasis-associated lung adenocarcinoma transcript 1 (*MALAT1*)/yes-associated protein (YAP) signaling pathway is involved in mediating apoptosis, particularly in tumor cells (36). Zhou *et al* (36) have demonstrated that the *MALAT1*/YAP signaling pathway is activated in pancreatic cancer cells, whereas downregulation of *MALAT1* suppresses the development of pancreatic cancer by inhibiting the Hippo/YAP signaling pathway and affecting apoptosis, which may be attributed to the inhibition of YAP translocation from the nucleus to the cytoplasm (37). Therefore, whether artesunate exhibits antitumor effects by regulating the *MALAT1*/YAP signaling pathway warrants further study.

The present study aimed to determine the effects of artesunate on the proliferation of UM cells and to explore the underlying mechanism. First, the effects of artesunate treatment on C918 cell proliferation and apoptosis were assessed. In addition, the role of the *MALAT1*/YAP axis in mediating the effects of artesunate was evaluated. Furthermore, the present study tested whether combination therapy was more efficient compared with single treatment, and described a potential novel strategy for treating UM in the clinic.

Materials and methods

Cell culture and chemicals. The human UM cell lines C918 and M619 were obtained from the Type Culture Collection of the Chinese Academy of Medical Sciences. C918 or M619 cells were incubated in DMEM (cat. no. C11995500BT; Gibco; Thermo Fisher Scientific, Inc.) supplemented with 10% fetal bovine serum (cat. no. P30-3301; PAN-Biotech GmbH) and 1% penicillin-streptomycin (cat. no. 15140-122; Gibco; Thermo Fisher Scientific, Inc.). All cells were maintained in an incubator at 37˚C with 5% CO_2 in a water-saturated atmosphere. Artesunate (Fig. 1A) and verteporfin were procured from Selleck Chemicals (cat. nos. S2265 and S1786, respectively) and used to treat the cells for 48 h. Dimethyl sulfoxide (DMSO; cat. no. 276855; Sigma-Aldrich; Merck KGaA) was used as a negative control.

Cell viability assay. Methyl thiazolyl tetrazolium (MTT) assays were used to analyze cell viability in the present study. C918 or M619 cells ($1x10^4$ cells/well) were cultured in 96-well plates at 37˚C with 5% CO_2. Following treatment with artesunate (0, 10, 20 and 40 μM) or a drug combination (40 μM artesunate and 5 μM verteporfin), MTT reagent (cat. no. M1020; Beijing Solarbio Science & Technology Co., Ltd.) was added to each well and incubated for 4 h at 37˚C. A microplate reader was used to measure absorbance at 490 nm. Experiments were repeated three times.

Caspase activity assay. C918 cells were plated at a density of $1x10^6$ cells/well in 6-well plates. Following treatment with artesunate (0, 10, 20 and 40 μM) or a drug combination (40 μM artesunate and 5 μM verteporfin), cells were lysed using RIPA buffer (cat. no. R0020, Beijing Solarbio Science & Technology Co., Ltd.), and protein concentration was determined using a commercial BCA kit (cat. no. P1511-1; Applygen Technologies, Inc.). Caspase-3 and caspase-9 activity levels were detected using Caspase3 and Caspase9 Activity kits (cat. nos. BC3830 and BC3890, respectively; Beijing Solarbio Science & Technology Co., Ltd.) according to the manufacturer's instructions. Absorbance of the resulting solution at 405 nm was determined using a microplate reader.

ROS level detection. C918 cells were exposed to various concentrations (0, 10, 20, and 40 μM) of artesunate for 48 h and resuspended in culture medium (without serum) containing 10 μM DCFH-DA (cat. no. CA1410; Beijing Solarbio Science & Technology Co., Ltd.) (38). The cells were harvested, and a microplate reader was used to detect the relative level of ROS at 488 and 525 nm. Cells treated with DMSO served as the negative control.

Lactate dehydrogenase (LDH) release assay. C918 cells ($1x10^4$ cells/well) were seeded into 96-well plates and subsequently treated with 0, 10, 20 and 40 μM artesunate for 48 h at 37˚C. LDH assays were performed using a commercial assay kit (cat. no. BC0685; Beijing Solarbio Science & Technology Co., Ltd.), according to the manufacturer's protocol.

ELISA. Following treatment with artesunate (0, 10, 20 and 40 μM) or a drug combination (40 μM artesunate and 5 μM

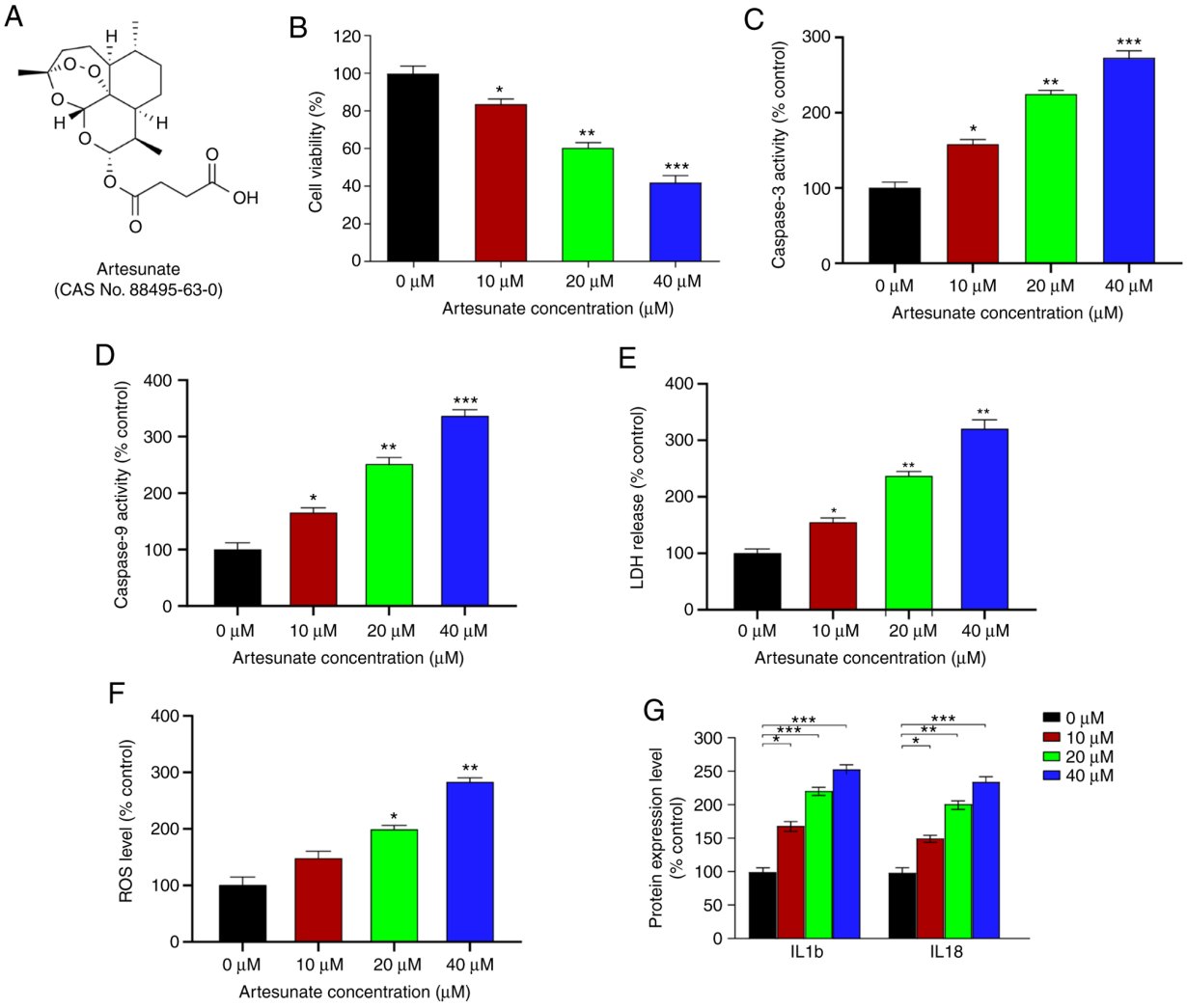

Figure 1. Artesunate inhibits the viability of C918 cells by enhancing apoptosis. (A) Structure of artesunate. (B) Viability of C918 cells following treatment with artesunate. The activity of (C) caspase-3 and (D) caspase-9 in C918 cells following artesunate treatment. Relative (E) intracellular ROS levels and (F) LDH release of C918 cells following artesunate treatment. (G) ELISA of IL-1β and IL-18 in C918 cells following artesunate administration. *P<0.05, **P<0.01 and ***P<0.001 vs. 0 μM. ROS, reactive oxygen species; LDH, lactate dehydrogenase.

verteporfin), C918 cells were lysed in RIPA lysis buffer (cat. no. R0020; Beijing Solarbio Science & Technology Co., Ltd.). The lysates were centrifuged at 12,000 x g for 30 min at 4˚C, and the supernatants were collected. Then, the concentrations of IL-1b and IL18 were determined using ELISA kits, according to the accompanying instructions (cat. nos. ab214025 and ab215539; Abcam). Absorption was determined using a microplate reader, and experiments were repeated three times.

Reverse transcription-quantitative (RT-q) PCR assay. Relative levels of target RNA were determined following treatment with artesunate (0, 10, 20 and 40 μM) or a drug combination (40 μM artesunate and 5 μM verteporfin). Total RNA of C918 cells was extracted from cells using TRIzol® reagent (cat. no. 15596-026; Invitrogen; Thermo Fisher Scientific, Inc.) according to the manufacturer's instructions, and the concentration of the extracted RNA was measured using a NanoDrop2000 (Thermo Fisher Scientific, Inc.). Subsequently, RNA was reverse-transcribed into cDNA using a reverse transcription kit (cat. no. 04896866001; Roche Molecular Systems, Inc.). SYBR® Green (TransGen Biotech Co., Ltd.) was used to perform RT-qPCR on the ABI-Quant Studio 5 system (Thermo Fisher Scientific, Inc.) to determine the relative expression levels of the target genes. Relative expression level of *YAP* was normalized to β-actin, and *MALAT1* was normalized to *U6*. The primer pairs used in this study are listed in the Table SI. The thermocycling conditions were as follows: Activation at 95˚C for 10 min; 40 cycles of denaturation at 95˚C for 30 sec, annealing at 60˚C for 30 sec (data collected during each cycle) and extension at 72˚C for 30 sec; and a melting curve between 55˚C and 95˚C (data collected at each temperature).

Cell transfection. Plasmids overexpressing *YAP* and *MALAT1* (constructed in pEGFP-N2) and negative controls (empty pEGFP-N2 vector) were synthesized by Shanghai GenePharma Co., Ltd.. Cells were transfected with 2 μg plasmid using Lipofectamine® 2000 transfection reagent (cat. no. 11668-027, Invitrogen; Thermo Fisher Scientific, Inc.) according to the manufacturer's instructions and cultured for 72 h at 37˚C. Subsequently, cells were harvested for further analysis.

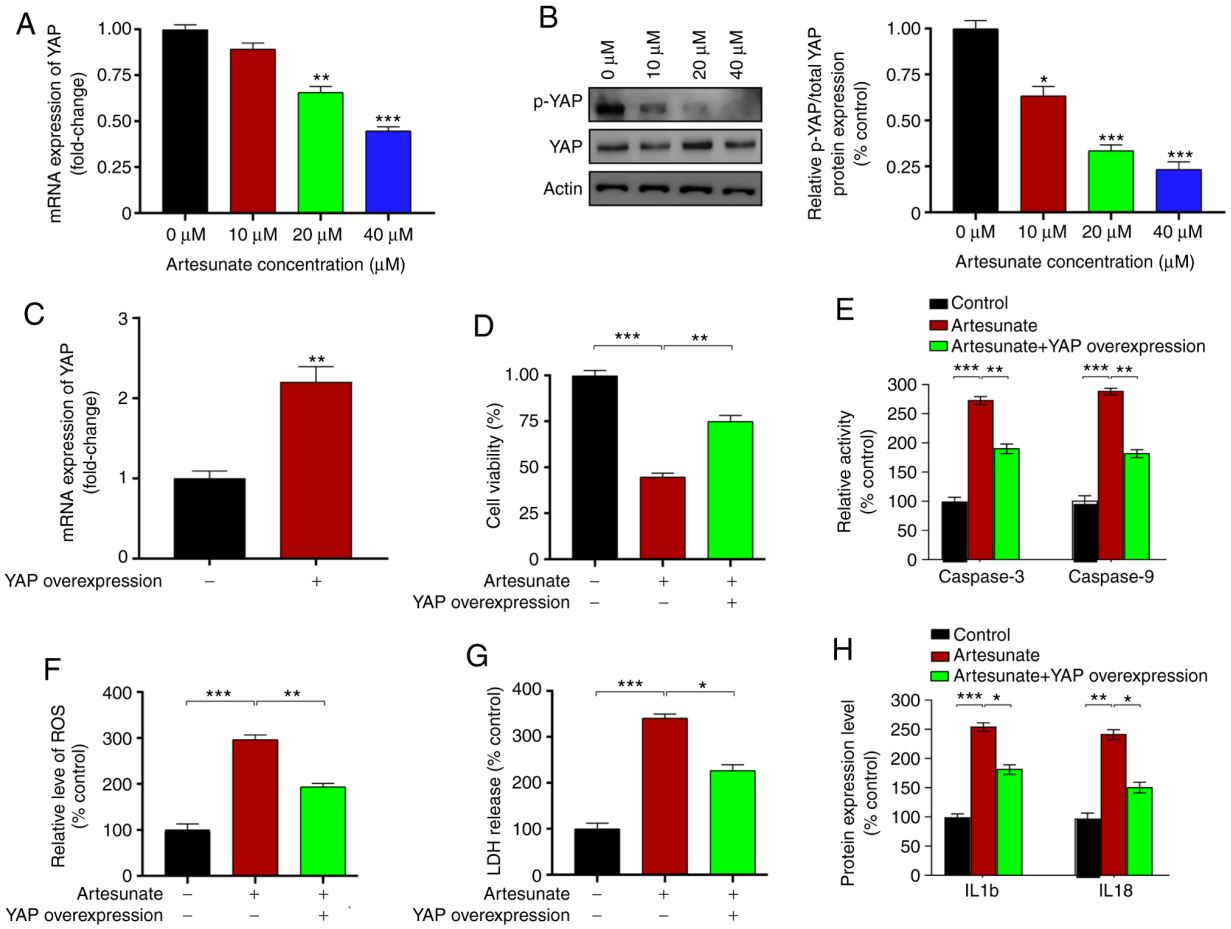

Figure 2. Artesunate-induced apoptosis is mediated by YAP. (A) qPCR analysis of the relative YAP mRNA levels in C918 cells normalized to those of β-actin. **P<0.01 and ***P<0.001 vs. 0 μM. (B) Representative western blot assay of phosphorylated and total YAP in C918 cells. *P<0.01 and ***P<0.001 vs. 0 μM. (C) qPCR analysis of the relative YAP mRNA levels following YAP overexpression plasmid transfection. **P<0.01 vs. negative control. (D) Viability of C918 cells following transfection. (E) Caspase-3 and caspase-9 activity in C918 cells following transfection. Relative (F) ROS levels and (G) LDH release of C918 cells following transfection. (H) ELISA of IL-1β and IL-18 levels in C918 following transfection. *P<0.05, **P<0.01 and ***P<0.001. YAP, yes-associated protein; qPCR, quantitative PCR; ROS, reactive oxygen species; LDH, lactate dehydrogenase; p-, phosphorylated.

Western blot assay. Following treatment with artesunate (0, 10, 20 and 40 μM) or overexpression plasmids, C918 cells were lysed on ice using RIPA lysis buffer (cat. no. R0020, Beijing Solarbio Science & Technology Co., Ltd.). The lysates were centrifuged at 12,000 x g for 30 min at 4˚C, the supernatants were collected, and total protein concentration was determined using a BCA quantitation kit (cat. no. P1511-1; Applygen Technologies, Inc.). Proteins were separated by 10% SDS-PAGE and transferred to PVDF membranes (cat. no. IPVH00010; MilliporeSigma). Following blocking with 5% milk at room temperature for 2 h, the membranes were incubated with primary antibodies at 4˚C overnight. Following three washes with 0.1% TBS-Tween 20, the membranes were incubated with secondary HRP-conjugated antibodies at room temperature for 2 h. ECL High-Signal reagent (170-5060; Bio-Rad Laboratories, Inc.) was used to visualize protein bands on a Bio-Rad System (Bio-Rad Laboratories, Inc.). β-actin served as a loading control. The primary antibodies were diluted 1:2,000, and the secondary antibodies were diluted 1:5,000. The antibody against YAP (cat. no. ab76252) was obtained from Abcam, and the actin antibody (cat. no. AC026) was purchased from ABclonal Biotech Co., Ltd. Secondary antibodies were obtained from Suzhou Biodragon Immunotechnologies Co., Ltd..

Statistical analysis. Data are presented as the mean ± SEM of ≥3 independent experiments for each assay. All experimental data were analyzed using SPSS software (version 24.0; IBM Corp.). Data were evaluated using an unpaired two-tailed Student's t-test or one-way analysis of variance followed by Bonferroni (for data meeting homogeneity of variance) or Tamhane's T2 (for data demonstrating heteroscedasticity) post hoc tests. P<0.05 was considered to indicate a statistically significant difference.

Results

Artesunate alleviates UM cell apoptosis and inflammation, and inhibits UM cell viability. Previous studies have demonstrated that artesunate reduces the number of viable C2C12 cells in a dose-dependent manner following a 48-h treatment (23). Therefore, the present study tested whether artesunate (Fig. 1A) exerted similar effects in UM cells. The results demonstrated that, relative to that in the control group, artesunate significantly reduced the viability of C918 cells, particularly at doses ≥10 μM (Fig. 1B). The effects of artesunate on M619 cells were also determined, and similar inhibition of cell viability was observed (Fig. S1). Due to more

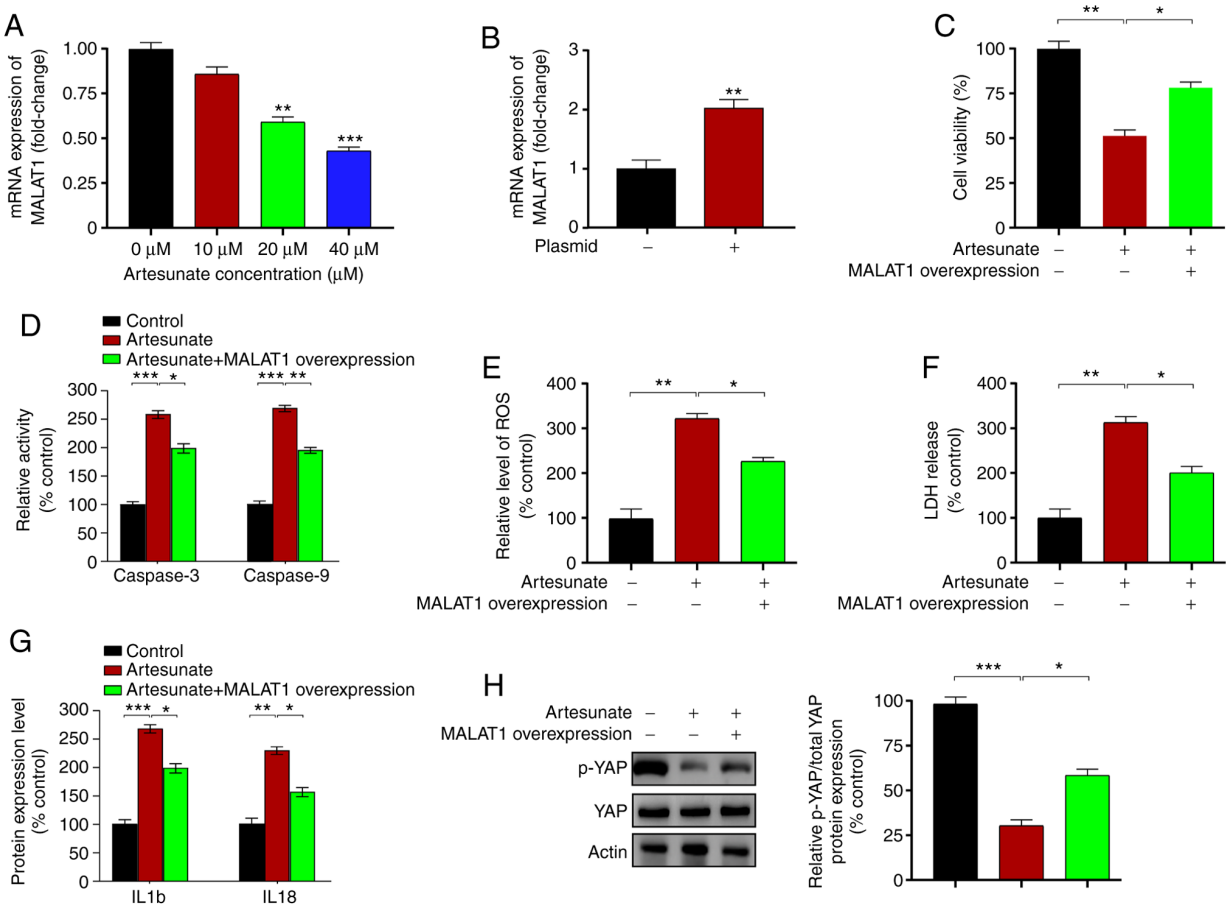

Figure 3. Artesunate-induced apoptosis in C918 cells is partially inhibited by MALAT1 overexpression. (A) Expression levels of *MALAT1* in C918 cells following treatment with artesunate. **P<0.01 and ***P<0.001 vs. 0 μM. (B) qPCR analysis of the relative MALAT1 levels following *MALAT1* overexpression plasmid transfection. **P<0.01 vs. negative control. (C) Viability of C918 cells following transfection with a plasmid overexpressing *MALAT1*. (D) Caspase-3 and caspase-9 activity in C918 cells following transfection. Analysis of (E) ROS levels and (F) LDH release in C918 cells following transfection with a *MALAT1* overexpression plasmid. (G) ELISA of IL-1β and IL-18 levels in C918 cells transfected with a *MALAT1* overexpression plasmid. (H) Western blotting images and quantified data of phosphorylated and total YAP in C918 cells following transfection with a MALAT1 overexpression plasmid. *P<0.05, **P<0.01 and ***P<0.001. *MALAT1*, metastasis-associated lung adenocarcinoma transcript 1; qPCR, quantitative PCR; ROS, reactive oxygen species; LDH, lactate dehydrogenase; YAP, yes-associated protein.

pronounced inhibitory effects of artesunate on C918 cells compared with those on M619 cells, this cell line was selected for further experiments.

The caspase-3 and caspase-9 activity levels were significantly increased in C918 cells following treatment with artesunate (Fig. 1C and D). In addition, cells treated with artesunate exhibited elevated ROS levels and LDH release compared with those in the control group (Fig. 1E and F). Furthermore, the effects of artesunate on the expression levels of inflammatory factors IL1b and IL18, which are positively associated with apoptosis (39), were assessed. Compared with those in the control cells, the levels of IL1b and IL18 were significantly increased following artesunate treatment (Fig. 1G), which suggested that artesunate exerted a proinflammatory effect on C918 cells. Overall, these results demonstrated that artesunate induced elevated apoptosis and an enhanced the inflammatory response, particularly at 40 μM, resulting in inhibition of C918 cell viability. Therefore, 40 μM artesunate was selected for use in further experiments.

Overexpression of YAP ameliorates the effects of artesunate in C918 cells. YAP is a crucial factor in UM progression (40). Therefore, the present study assessed whether may YAP serve a role in mediating the effects of artesunate on UM cell apoptosis. Cells were treated with 40 μM artesunate for 48 h. The results of qPCR and western blot assays demonstrated that YAP expression and phosphorylation levels were significantly decreased following artesunate treatment compared with those in the control cells (Fig. 2A and B). Subsequently, C918 cells were transfected with a plasmid overexpressing YAP to assess the role of YAP in mediating the effects of artesunate. Plasmid transfection significantly enhanced the expression levels of YAP compared with those in the cells transfected with the empty vector (Fig. 2C). Compared with cells treated with artesunate alone, those overexpressing YAP exhibited reversal of the inhibitory effects of artesunate, as elevated C918 cell viability was observed (Fig. 2D). In addition, the caspase-3 and caspase-9 activity levels were decreased following YAP overexpression compared with those in control cells treated with artesunate (Fig. 2E). YAP overexpression plasmid transfection also reduced the levels of intracellular ROS and LDH release (Fig. 2F and G), which were accompanied by decreased levels of IL1b and IL18 (Fig. 2H) compared with those in artesunate-treated control cells. Overall, these results

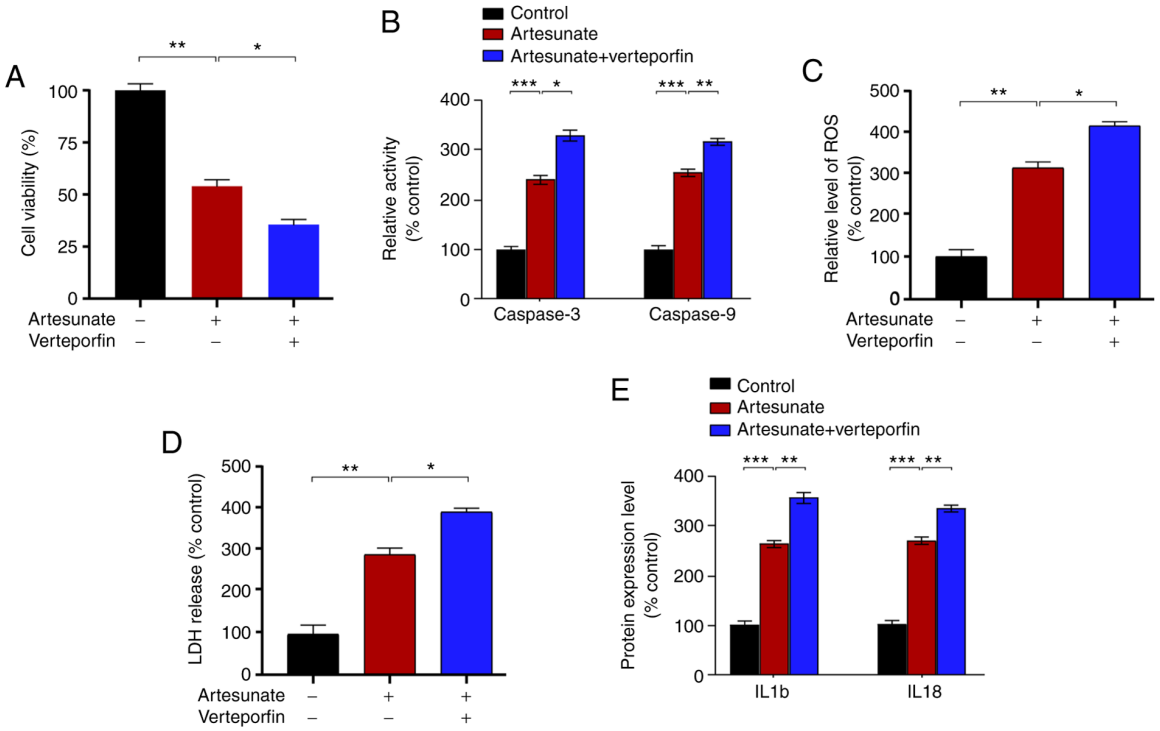

Figure 4. Combined therapy is more efficient at enhancing apoptosis in C918 cells compared with artesunate alone. (A) Viability, (B) caspase-3 and caspase-9 activity, (C) ROS levels, (D) LDH release and (E) ELISA of IL-1β and IL-18 levels of C918 cells following treatment with artesunate or combined therapy. *P<0.05, **P<0.01 and ***P<0.001. ROS, reactive oxygen species; LDH, lactate dehydrogenase.

demonstrated that YAP was involved in mediating C918 cell apoptosis induced by artesunate.

Upregulation of MALAT1 reverses the effects of artesunate by regulating YAP levels in C918 cells. The present study next analyzed the effects of artesunate treatment on the upstream regulator of YAP *MALAT1*, which binds to the pro-metastatic transcription factor TEA domain (TEAD), blocking TEAD from associating with its coactivator YAP (41). The results demonstrated that artesunate significantly downregulated the mRNA expression levels of *MALAT1* in C918 cells compared with those in the control group (Fig. 3A). *MALAT1* was overexpressed by transfecting a plasmid into C918 cells, which significantly enhanced the expression levels of *MALAT1* compared with those in the empty vector-transfected cells (Fig. 3B). Compared with those in the control C918 cells treated with artesunate alone, *MALAT1* overexpression led to increased cell viability (Fig. 3C), reduced caspase-3 and caspase-9 activity levels (Fig. 3D), and decreased levels of LDH release and intracellular ROS (Fig. 3E and F). In addition, the levels of IL1b and IL18 were assessed following transfection and were significantly reduced following *MALAT1* overexpression in C918 cells compared with those in the control cells treated with artesunate (Fig. 3G). Notably, YAP phosphorylation levels were upregulated in response to *MALAT1* overexpression compared with those in the control cells treated with artesunate (Fig. 3H). These results suggested that *MALAT1*/YAP signaling may serve an important role in mediating the effects of artesunate on C918 cells.

Verteporfin enhances the antitumor effects of artesunate in C918 cells. The present study further assessed the ability of combination therapy to treat UM. Combination therapy has strong potential for application in clinical treatment of diseases, such as diabetes (42), glioblastoma (43), and rheumatoid arthritis (44), as well as various types of tumor (45-47). As an inhibitor of YAP, verteporfin suppresses the interaction between YAP and TEAD (48). Therefore, the present study determined the effects of combined artesunate and verteporfin treatment in C918 cells. The results demonstrated that verteporfin enhanced the inhibitory effects of artesunate on C918 cells, further inhibiting cell viability (Fig. 4A), elevating caspase-3 and caspase-9 activity levels (Fig. 4B), and increasing intracellular ROS and LDH release (Fig. 4C and D) compared with those in the cells treated with artesunate alone. In addition, combination therapy significantly increased the levels of IL18 and IL1b compared with those following treatment with artesunate alone (Fig. 4E). In conclusion, combination therapy exerted stronger effects on C918 cells compared with treatment with artesunate alone.

Discussion

UM is a primary malignant intraocular tumor in adults, which represents 5-6% of all melanoma diagnoses (49); however, effective therapies for UM are lacking, although certain advances have been achieved in local ocular treatments, such as chemotherapy and immunotherapy (50). In addition, various small molecules have been demonstrated to exhibit potent antitumor activity *in vivo* and *in vitro*, including sorafenib (51), crotepoxide (52) and luteolin (53). Notably, combination therapies exhibit higher efficacy compared with single-treatment approaches (54,55). For instance, Matsunaga *et al* (55) have

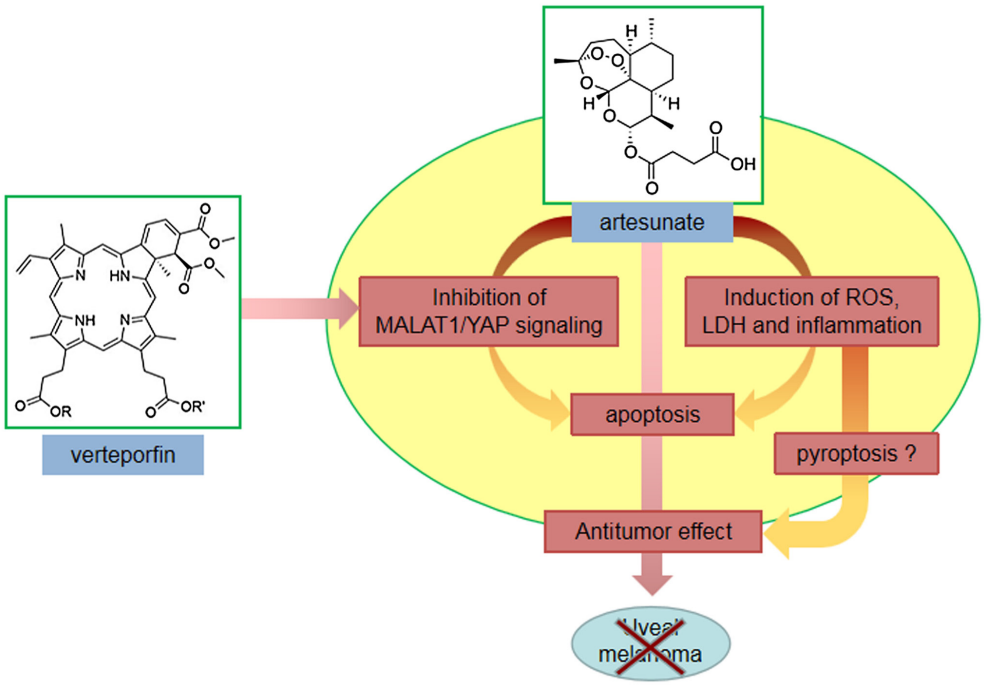

Figure 5. Schematic diagram of the molecular mechanism underlying *MALAT1*-mediated inactivation of YAP signaling in the inhibition of uveal melanoma cell viability. YAP, yes-associated protein; *MALAT1*, metastasis-associated lung adenocarcinoma transcript 1; ROS, reactive oxygen species; LDH, lactate dehydrogenase.

demonstrated that combination therapy exhibits higher treatment efficacy for Alzheimer's disease compared with that of a single cholinesterase inhibitor. In the present study, artesunate was identified as a potential candidate to inhibit UM cell viability by enhancing apoptosis. Furthermore, the results of the present study demonstrated that the *MALAT1*/YAP signaling pathway was involved in mediating the effects of artesunate. In addition, verteporfin enhanced the artesunate treatment-mediated induction of apoptosis in C918 cells, providing evidence for its potential for application in treating UM.

ROS serves dual roles in biological processes, including the maintenance of normal physiological conditions, as well as exerting pathogenic effects by inducing cell damage and destruction during pathophysiology (56). Under physiological conditions, ROS preferentially triggers redox signaling rather than inducing oxidative damage to macromolecules, such as proteins, lipids and DNA (57); however, previous studies have suggested that ROS serves a crucial role in tumor proliferation and progression (57,58). Pelicano *et al* (59) have demonstrated that moderate mitochondrial ROS levels promote breast cancer cell motility in a CXCL14-dependent manner. Notably, a positive association has also been identified between apoptosis and ROS production (60,61). Similar to previous reports (35,62), the results of the present study revealed that artesunate induced apoptosis in a ROS-dependent manner. In addition, the present study demonstrates that overexpression of *MALAT1* or YAP reversed the antitumor effects of artesunate on ROS induction and apoptosis in C918 cells, indicating that *MALAT1* or YAP may be potential drug targets for UM treatment.

YAP is a transcriptional coactivator that shuttles between the cytoplasm and the nucleus (63). YAP recognizes cognate cis-regulatory elements by interacting with other transcription factors in the nucleus, particularly TEAD family members (64). As a transcriptional regulator of TEAD, YAP activates the transcription of genes involved in cell proliferation, leading to a suppression of apoptosis (65). YAP is regulated by the Hippo signaling pathway to control tumor progression (66). In addition, YAP is an oncogene and serves crucial roles in various types of human cancer (65,67), such as kidney and blood cancer (68,69). White *et al* (68) have reported that inhibition of the YAP/TAZ signaling pathway suppresses glycolysis-dependent proliferation and enhances mitochondrial respiration as well as ROS buildup, resulting in the death of kidney tumor cells when challenged by nutrient stress. Additionally, neratinib suppresses the proliferation of pancreatic and blood cancer cells by inhibiting the Hippo/YAP signaling pathway and mutant KRAS expression (69). Neratinib upregulates the phosphorylation of YAP and TAZ by 30% and promotes YAP translocation into the cytosol, resulting in a reduction of YAP/TAZ protein levels. In addition, knockdown of YAP enhances the lethality of neratinib (69). These previous studies indicate that YAP serves a crucial role in mediating the antitumor effects of small molecules by regulating apoptosis. Notably, a previous study has demonstrated an activation of YAP in UM compared with that in patients without metastasis (70). Therefore, as an enhanced effect of artesunate on UM cell apoptosis was observed in the present study, we hypothesized that YAP may be involved in mediating the effects of artesunate in C918 cells. The results of the present study demonstrated that artesunate treatment significantly reduced YAP expression. Furthermore, YAP overexpression ameliorated the inhibitory effects of artesunate in C918 cells, reducing caspase-3 and caspase-9 activity levels, as well as inhibiting the levels of IL1b and IL18. Compared with those in the control group, artesunate treatment led to elevated levels of IL1b and IL18 in C918 cells, whereas previous

studies have reported that it exerts an anti-inflammatory effect (71,72). This may be attributed to enhanced of caspase-1 activity, which is a factor upstream of pyroptosis (73). In the present study, caspase-1 activity was increased following artesunate treatment compared with that in the control cells (data not shown). During the process of pyroptosis, caspase-1 specifically cleaves the linker between the N- and C-terminal domains of gasdermin D (GSDMD), leading to release of GSDMD N-terminal domain (74). GSDMD is an executor of pyroptosis and is required for the secretion of IL1β and IL18 (75). Additionally, YAP is a suppressor of inflammation (76); thus, a high level of inflammation may be associated with low YAP expression levels. In our future studies, the effects of artesunate on the regulation of pyroptosis in UM cells will be assessed.

As an infrequently spliced non-coding RNA, *MALAT1* is highly conserved amongst mammals and strongly expressed in the nucleus (77). *MALAT1* contributes to various physiological processes, including alternative splicing, nuclear organization, and epigenetic modulation of gene expression (78). In addition, previous studies have provided evidence that *MALAT1* is crucial for the regulation of tumor cell proliferation. For example, methyltransferase-like 3 initiates m6A mRNA methylation and promotes *YAP* mRNA translation by regulating the *MALAT1*/microRNA (miR)-1914-3p/YAP axis, which increases *YAP* mRNA stability and induces non-small cell lung cancer drug resistance and metastasis (79). In addition, Sun *et al* (80) have reported that silencing of *MALAT1* upregulates miR-181a-5p levels by activating the Hippo-YAP signaling pathway, leading to inhibition of myeloma cell proliferation and adhesion. These results suggest an association between YAP and *MALAT1* in the regulation of tumor cell proliferation (81). Therefore, the present study aimed to determine how *MALAT1* may contribute to mediating the effects of artesunate, since YAP expression levels were reduced in response to artesunate treatment. The results demonstrated that artesunate suppressed C918 cell viability by inhibiting the *MALAT1*/YAP signaling pathway, whereas the inhibitory effect was ameliorated by *MALAT1* overexpression, which supported the role of the *MALAT1*/YAP axis in mediating the effects of artesunate on UM cells. The present study also assessed the feasibility of combination therapy for UM. Compared with cells treated with artesunate alone, cells administered a combination of artesunate and verteporfin exhibited lower viability and higher levels of apoptosis, indicating that combination therapy may be more effective.

However, there were certain limitations to the present study. For instance, the present study did not assess whether artesunate may alleviate UM by regulating the *MALAT1*/YAP signaling pathway in a mouse UM model. Additionally, how pyroptosis is involved in mediating the effects of artesunate remains elusive. In the future, multiple cell lines will be used to verify the results of the present study, and the antitumor effects of artesunate will be analyzed in animal models of UM. In addition, other drugs with the potential to inhibit UM cell proliferation will be assessed, with the aim of advancing UM treatment in the clinic.

In conclusion, the results of the present study identified artesunate as a potent small molecule that inhibited UM cell proliferation. In addition, the *MALAT1*/YAP signaling pathway was demonstrated to mediate the effects of artesunate. Notably, combination therapy exerted a stronger inhibitory effect on C918 cells compared with treatment with artesunate alone (Fig. 5). To the best of our knowledge, this is the first report of assessment of the role of *MALAT1*/YAP signaling in mediating the effects of artesunate in UM cells, and it provides evidence supporting artesunate combined with verteporfin as a candidate clinical treatment for UM.

Acknowledgements

Not applicable.

Funding

No funding was received.

Availability of data and materials

The datasets used and/or analyzed during the current study are available from the corresponding author on reasonable request.

Authors' contributions

JW and XJ designed and performed the study, analyzed the data and wrote the manuscript. YL contributed to the writing the manuscript and data analysis. JW, XJ and YL confirm the authenticity of all the raw data. All authors read and approved the final manuscript.

Ethics approval and consent to participate

Not applicable.

Patient consent for publication

Not applicable.

Competing interests

The authors declare that they have no competing interests.

References

1. McLaughlin CC, Wu XC, Jemal A, Martin HJ, Roche LM and Chen VW: Incidence of noncutaneous melanomas in the U.S. Cancer 103: 1000-1007, 2005.
2. Ortega MA, Fraile-Martinez O, Garcia-Honduvilla N, Álvarez-Mon M, Buján J and Teus MA: Update on uveal melanoma: Translational research from biology to clinical practice (review). Int J Oncol 57: 1262-1279, 2020.
3. Landreville S, Agapova OA and Harbour JW: Emerging insights into the molecular pathogenesis of uveal melanoma. Future Oncol 4: 629-636, 2008.
4. Singh AD, Bergman L and Seregard S: Uveal melanoma: Epidemiologic aspects. Ophthalmol Clin North Am 18: 75-84, viii, 2005.
5. Chandran SS, Somerville RPT, Yang JC, Sherry RM, Klebanoff CA, Goff SL, Wunderlich JR, Danforth DN, Zlott D, Paria BC, *et al*: Treatment of metastatic uveal melanoma with adoptive transfer of tumour-infiltrating lymphocytes: A single-centre, two-stage, single-arm, phase 2 study. Lancet Oncol 18: 792-802, 2017.

6. Basile MS, Mazzon E, Russo A, Mammana S, Longo A, Bonfiglio V, Fallico M, Caltabiano R, Fagone P, Nicoletti F, *et al*: Differential modulation and prognostic values of immune-escape genes in uveal melanoma. PLoS One 14: e0210276, 2019.
7. Petralia MC, Mazzon E, Fagone P, Russo A, Longo A, Avitabile T, Nicoletti F, Reibaldi M and Basile MS: Characterization of the pathophysiological role of CD47 in uveal melanoma. Molecules 24: 2450, 2019.
8. Basile MS, Mazzon E, Fagone P, Longo A, Russo A, Fallico M, Bonfiglio V, Nicoletti F, Avitabile T and Reibaldi M: Immunobiology of uveal melanoma: State of the art and therapeutic targets. Front Oncol 9: 1145, 2019.
9. Naing A, Papadopoulos KP, Autio KA, Ott PA, Patel MR, Wong DJ, Falchook GS, Pant S, Whiteside M, Rasco DR, *et al*: Safety, antitumor activity, and immune activation of pegylated recombinant human interleukin-10 (AM0010) in patients with advanced solid tumors. J Clin Oncol 34: 3562-3569, 2016.
10. Parker T, Rigney G, Kallos J, Stefko ST, Kano H, Niranjan A, Green AL, Aziz T, Rath P and Lunsford LD: Gamma knife radiosurgery for uveal melanomas and metastases: A systematic review and meta-analysis. Lancet Oncol 21: 1526-1536, 2020.
11. Selumetinib shows promise in metastatic uveal melanoma. Cancer Discov 3: OF8, 2013.
12. Pelster MS, Gruschkus SK, Bassett R, Gombos DS, Shephard M, Posada L, Glover MS, Simien R, Diab A, Hwu P, *et al*: Nivolumab and ipilimumab in metastatic uveal melanoma: Results from a single-arm phase II study. J Clin Oncol 39: 599-607, 2021.
13. Carvajal RD, Piperno-Neumann S, Kapiteijn E, Chapman PB, Frank S, Joshua AM, Piulats JM, Wolter P, Cocquyt V, Chmielowski B, *et al*: Selumetinib in combination with dacarbazine in patients with metastatic uveal melanoma: A phase III, multicenter, randomized trial (SUMIT). J Clin Oncol 36: 1232-1239, 2018.
14. Judd R, Bagley MC, Li M, Zhu Y, Lei C, Yuzuak S, Ekelöf M, Pu G, Zhao X, Muddiman DC and Xie DY: Artemisinin biosynthesis in non-glandular trichome cells of artemisia annua. Mol Plant 12: 704-714, 2019.
15. Dondorp AM, Fanello CI, Hendriksen IC, Gomes E, Seni A, Chhaganlal KD, Bojang K, Olaosebikan R, Anunobi N, Maitland K, *et al*: Artesunate versus quinine in the treatment of severe falciparum malaria in African children (AQUAMAT): An open-label, randomised trial. Lancet 376: 1647-1657, 2010.
16. Vivas L, Rattray L, Stewart L, Bongard E, Robinson BL, Peters W and Croft SL: Anti-malarial efficacy of pyronaridine and artesunate in combination in vitro and in vivo. Acta Trop 105: 222-228, 2008.
17. Zeng XZ, Zhang YY, Yang Q, Wang S, Zou BH, Tan YH, Zou M, Liu SW and Li XJ: Artesunate attenuates LPS-induced osteoclastogenesis by suppressing TLR4/TRAF6 and PLCγ1-Ca^{2+}-NFATc1 signaling pathway. Acta Pharmacol Sin 41: 229-236, 2020.
18. Uzun T, Toptas O, Saylan A, Carver H and Turkoglu SA: Evaluation and comparison of the effects of artesunate, dexamethasone, and tacrolimus on sciatic nerve regeneration. J Oral Maxillofac Surg 77: 1092.e1-1092.e12, 2019.
19. Vatsveen TK, Myhre MR, Steen CB, Wälchli S, Lingjærde OC, Bai B, Dillard P, Theodossiou TA, Holien T, Sundan A, *et al*: Artesunate shows potent anti-tumor activity in B-cell lymphoma. J Hematol Oncol 11: 23, 2018.
20. Ishikawa C, Senba M and Mori N: Evaluation of artesunate for the treatment of adult T-cell leukemia/lymphoma. Eur J Pharmacol 872: 172953, 2020.
21. Roh JL, Kim EH, Jang H and Shin D: Nrf2 inhibition reverses the resistance of cisplatin-resistant head and neck cancer cells to artesunate-induced ferroptosis. Redox Biol 11: 254-262, 2017.
22. Yao X, Zhao CR, Yin H, Wang K and Gao JJ: Synergistic antitumor activity of sorafenib and artesunate in hepatocellular carcinoma cells. Acta Pharmacol Sin 41: 1609-1620, 2020.
23. Chen S, Gan S, Han L, Li X, Xie X, Zou D and Sun H: Artesunate induces apoptosis and inhibits the proliferation, stemness, and tumorigenesis of leukemia. Ann Transl Med 8: 767, 2020.
24. Beccafico S, Morozzi G, Marchetti MC, Riccardi C, Sidoni A, Donato R and Sorci G: Artesunate induces ROS- and p38 MAPK-mediated apoptosis and counteracts tumor growth in vivo in embryonal rhabdomyosarcoma cells. Carcinogenesis 36: 1071-1083, 2015.
25. Zheng L and Pan J: The anti-malarial drug artesunate blocks Wnt/β-catenin pathway and inhibits growth, migration and invasion of uveal melanoma cells. Curr Cancer Drug Targets 18: 988-998, 2018.
26. Berger TG, Dieckmann D, Efferth T, Schultz ES, Funk JO, Baur A and Schuler G: Artesunate in the treatment of metastatic uveal melanoma-first experiences. Oncol Rep 14: 1599-1603, 2005.
27. Elmore S: Apoptosis: A review of programmed cell death. Toxicol Pathol 35: 495-516, 2007.
28. Lin J, Zhang D, Fan Y, Chao Y, Chang J, Li N, Han L and Han C: Regulation of cancer stem cell self-renewal by HOXB9 antagonizes endoplasmic reticulum stress-induced melanoma cell apoptosis via the miR-765-FOXA2 axis. J Invest Dermatol 138: 1609-1619, 2018.
29. Roberti MP, Yonekura S, Duong CPM, Picard M, Ferrere G, Tidjani Alou M, Rauber C, Iebba V, Lehmann CHK, Amon L, *et al*: Chemotherapy-induced ileal crypt apoptosis and the ileal microbiome shape immunosurveillance and prognosis of proximal colon cancer. Nat Med 26: 919-931, 2020.
30. Singh A, Sweeney MF, Yu M, Burger A, Greninger P, Benes C, Haber DA and Settleman J: TAK1 inhibition promotes apoptosis in KRAS-dependent colon cancers. Cell 148: 639-650, 2012.
31. Ogawa S, Fukuda A, Matsumoto Y, Hanyu Y, Sono M, Fukunaga Y, Masuda T, Araki O, Nagao M, Yoshikawa T, *et al*: SETDB1 inhibits p53-mediated apoptosis and is required for formation of pancreatic ductal adenocarcinomas in mice. Gastroenterology 159: 682-696.e13, 2020.
32. Reyna DE, Garner TP, Lopez A, Kopp F, Choudhary GS, Sridharan A, Narayanagari SR, Mitchell K, Dong B, Bartholdy BA, *et al*: Direct activation of BAX by BTSA1 overcomes apoptosis resistance in acute myeloid leukemia. Cancer Cell 32: 490-505.e10, 2017.
33. Nangia V, Siddiqui FM, Caenepeel S, Timonina D, Bilton SJ, Phan N, Gomez-Caraballo M, Archibald HL, Li C, Fraser C, *et al*: Exploiting MCL1 dependency with combination MEK + MCL1 inhibitors leads to induction of apoptosis and tumor regression in KRAS-mutant non-small cell lung cancer. Cancer Discov 8: 1598-1613, 2018.
34. Mao J, Tian Y, Wang C, Jiang K, Li R, Yao Y, Zhang R, Sun D, Liang R, Gao Z, *et al*: CBX2 regulates proliferation and apoptosis via the phosphorylation of YAP in hepatocellular carcinoma. J Cancer 10: 2706-2719, 2019.
35. Zhou X, Chen Y, Wang F, Wu H, Zhang Y, Liu J, Cai Y, Huang S, He N, Hu Z and Jin X: Artesunate induces autophagy dependent apoptosis through upregulating ROS and activating AMPK-mTOR-ULK1 axis in human bladder cancer cells. Chem Biol Interact 331: 109273, 2020.
36. Zhou Y, Shan T, Ding W, Hua Z, Shen Y, Lu Z, Chen B and Dai T: Study on mechanism about long noncoding RNA MALAT1 affecting pancreatic cancer by regulating Hippo-YAP signaling. J Cell Physiol 233: 5805-5814, 2018.
37. Wu X, Wang Y, Zhong W, Cheng H and Tian Z: The long non-coding RNA MALAT1 enhances ovarian cancer cell stemness by inhibiting YAP translocation from nucleus to cytoplasm. Med Sci Monit 26: e922012, 2020.
38. Wang C, Guan Y, Lv M, Zhang R, Guo Z, Wei X, Du X, Yang J, Li T, Wan Y, *et al*: Manganese increases the sensitivity of the cGAS-STING pathway for double-stranded DNA and is required for the host defense against DNA viruses. Immunity 48: 675-687.e7, 2018.
39. Van Opdenbosch N and Lamkanfi M: Caspases in cell death, inflammation, and disease. Immunity 50: 1352-1364, 2019.
40. Li H, Li Q, Dang K, Ma S, Cotton JL, Yang S, Zhu LJ, Deng AC, Ip YT, Johnson RL, *et al*: YAP/TAZ activation drives uveal melanoma initiation and progression. Cell Rep 29: 3200-3211.e4, 2019.
41. Kim J, Piao HL, Kim BJ, Yao F, Han Z, Wang Y, Xiao Z, Siverly AN, Lawhon SE, Ton BN, *et al*: Long noncoding RNA MALAT1 suppresses breast cancer metastasis. Nat Genet 50: 1705-1715, 2018.
42. Matthews DR, Paldanius PM, Proot P, Chiang Y, Stumvoll M and Del Prato S; VERIFY study group: Glycaemic durability of an early combination therapy with vildagliptin and metformin versus sequential metformin monotherapy in newly diagnosed type 2 diabetes (VERIFY): A 5-year, multicentre, randomised, double-blind trial. Lancet 394: 1519-1529, 2019.
43. Herrlinger U, Tzaridis T, Mack F, Steinbach JP, Schlegel U, Sabel M, Hau P, Kortmann RD, Krex D, Grauer O, *et al*: Lomustine-temozolomide combination therapy versus standard temozolomide therapy in patients with newly diagnosed glioblastoma with methylated MGMT promoter (CeTeG/NOA-09): A randomised, open-label, phase 3 trial. Lancet 393: 678-688, 2019.

44. Hazlewood GS, Barnabe C, Tomlinson G, Marshall D, Devoe D and Bombardier C: Methotrexate monotherapy and methotrexate combination therapy with traditional and biologic disease modifying antirheumatic drugs for rheumatoid arthritis: Abridged Cochrane systematic review and network meta-analysis. BMJ 353: i1777, 2016.
45. Wong PP, Demircioglu F, Ghazaly E, Alrawashdeh W, Stratford MR, Scudamore CL, Cereser B, Crnogorac-Jurcevic T, McDonald S, Elia G, *et al*: Dual-action combination therapy enhances angiogenesis while reducing tumor growth and spread. Cancer Cell 27: 123-137, 2015.
46. Chen Q, Feng L, Liu J, Zhu W, Dong Z, Wu Y and Liu Z: Intelligent albumin-MnO2 nanoparticles as pH-/H2 O2-responsive dissociable nanocarriers to modulate tumor hypoxia for effective combination therapy. Adv Mater 28: 7129-7136, 2016.
47. Jain RK: Normalizing tumor vasculature with anti-angiogenic therapy: A new paradigm for combination therapy. Nat Med 7: 987-989, 2001.
48. Wei H, Wang F, Wang Y, Li T, Xiu P, Zhong J, Sun X and Li J: Verteporfin suppresses cell survival, angiogenesis and vasculogenic mimicry of pancreatic ductal adenocarcinoma via disrupting the YAP-TEAD complex. Cancer Sci 108: 478-487, 2017.
49. Singh AD, Turell ME and Topham AK: Uveal melanoma: Trends in incidence, treatment, and survival. Ophthalmology 118: 1881-1885, 2011.
50. Alvarez-Rodriguez B, Latorre A, Posch C and Somoza A: Recent advances in uveal melanoma treatment. Med Res Rev 37: 1350-1372, 2017.
51. Liu L, Cao Y, Chen C, Zhang X, McNabola A, Wilkie D, Wilhelm S, Lynch M and Carter C: Sorafenib blocks the RAF/MEK/ERK pathway, inhibits tumor angiogenesis, and induces tumor cell apoptosis in hepatocellular carcinoma model PLC/PRF/5. Cancer Res 66: 11851-11858, 2006.
52. Prasad S, Yadav VR, Sundaram C, Reuter S, Hema PS, Nair MS, Chaturvedi MM and Aggarwal BB: Crotepoxide chemosensitizes tumor cells through inhibition of expression of proliferation, invasion, and angiogenic proteins linked to proinflammatory pathway. J Biol Chem 291: 16921, 2016.
53. Chian S, Thapa R, Chi Z, Wang XJ and Tang X: Luteolin inhibits the Nrf2 signaling pathway and tumor growth in vivo. Biochem Biophys Res Commun 447: 602-608, 2014.
54. Wilding JP: Combination therapy for obesity. J Psychopharmacol 31: 1503-1508, 2017.
55. Matsunaga S, Kishi T and Iwata N: Combination therapy with cholinesterase inhibitors and memantine for Alzheimer's disease: A systematic review and meta-analysis. Int J Neuropsychopharmacol 18: pyu115, 2014.
56. Mijatović S, Savić-Radojević A, Plješa-Ercegovac M, Simić T, Nicoletti F and Maksimović-Ivanić D: The double-faced role of nitric oxide and reactive oxygen species in solid tumors. Antioxidants (Basel) 9: 374, 2020.
57. Assi M: The differential role of reactive oxygen species in early and late stages of cancer. Am J Physiol Regul Integr Comp Physiol 313: R646-R653, 2017.
58. Sosa V, Moliné T, Somoza R, Paciucci R, Kondoh H and LLeonart ME: Oxidative stress and cancer: An overview. Ageing Res Rev 12: 376-390, 2013.
59. Pelicano H, Lu W, Zhou Y, Zhang W, Chen Z, Hu Y and Huang P: Mitochondrial dysfunction and reactive oxygen species imbalance promote breast cancer cell motility through a CXCL14-mediated mechanism. Cancer Res 69: 2375-2383, 2009.
60. Mao X, Yu CR, Li WH and Li WX: Induction of apoptosis by shikonin through a ROS/JNK-mediated process in Bcr/Abl-positive chronic myelogenous leukemia (CML) cells. Cell Res 18: 879-888, 2008.
61. Takahashi M, Higuchi M, Makokha GN, Matsuki H, Yoshita M, Tanaka Y and Fujii M: HTLV-1 Tax oncoprotein stimulates ROS production and apoptosis in T cells by interacting with USP10. Blood 122: 715-725, 2013.
62. Qin G, Wu L, Liu H, Pang Y, Zhao C, Wu S, Wang X and Chen T: Artesunate induces apoptosis via a ROS-independent and Bax-mediated intrinsic pathway in HepG2 cells. Exp Cell Res 336: 308-317, 2015.
63. Koo JH and Guan KL: Interplay between YAP/TAZ and metabolism. Cell Metab 28: 196-206, 2018.
64. Zanconato F, Cordenonsi M and Piccolo S: YAP/TAZ at the roots of cancer. Cancer Cell 29: 783-803, 2016.
65. Huang J, Wu S, Barrera J, Matthews K and Pan D: The Hippo signaling pathway coordinately regulates cell proliferation and apoptosis by inactivating yorkie, the drosophila homolog of YAP. Cell 122: 421-434, 2005.
66. Piccolo S, Dupont S and Cordenonsi M: The biology of YAP/TAZ: Hippo signaling and beyond. Physiol Rev 94: 1287-1312, 2014.
67. Overholtzer M, Zhang J, Smolen GA, Muir B, Li W, Sgroi DC, Deng CX, Brugge JS and Haber DA: Transforming properties of YAP, a candidate oncogene on the chromosome 11q22 amplicon. Proc Natl Acad Sci USA 103: 12405-12410, 2006.
68. White SM, Avantaggiati ML, Nemazanyy I, Di Poto C, Yang Y, Pende M, Gibney GT, Ressom HW, Field J, Atkins MB and Yi C: YAP/TAZ inhibition induces metabolic and signaling rewiring resulting in targetable vulnerabilities in NF2-deficient tumor cells. Dev Cell 49: 425-443.e9, 2019.
69. Dent P, Booth L, Roberts JL, Liu J, Poklepovic A, Lalani AS, Tuveson D, Martinez J and Hancock JF: Neratinib inhibits Hippo/YAP signaling, reduces mutant K-RAS expression, and kills pancreatic and blood cancer cells. Oncogene 38: 5890-5904, 2019.
70. Brouwer NJ, Konstantinou EK, Gragoudas ES, Marinkovic M, Luyten GPM, Kim IK, Jager MJ and Vavvas DG: Targeting the YAP/TAZ pathway in uveal and conjunctival melanoma with verteporfin. Invest Ophthalmol Vis Sci 62: 3, 2021.
71. Kumar VL, Verma S and Das P: Artesunate suppresses inflammation and oxidative stress in a rat model of colorectal cancer. Drug Dev Res 80: 1089-1097, 2019.
72. Feng FB and Qiu HY: Effects of artesunate on chondrocyte proliferation, apoptosis and autophagy through the PI3K/AKT/mTOR signaling pathway in rat models with rheumatoid arthritis. Biomed Pharmacother 102: 1209-1220, 2018.
73. Wang Y, Gao W, Shi X, Ding J, Liu W, He H, Wang K and Shao F: Chemotherapy drugs induce pyroptosis through caspase-3 cleavage of a gasdermin. Nature 547: 99-103, 2017.
74. Shi J, Zhao Y, Wang K, Shi X, Wang Y, Huang H, Zhuang Y, Cai T, Wang F and Shao F: Cleavage of GSDMD by inflammatory caspases determines pyroptotic cell death. Nature 526: 660-665, 2015.
75. He WT, Wan H, Hu L, Chen P, Wang X, Huang Z, Yang ZH, Zhong CQ and Han J: Gasdermin D is an executor of pyroptosis and required for interleukin-1β secretion. Cell Res 25: 1285-1298, 2015.
76. Lv Y, Kim K, Sheng Y, Cho J, Qian Z, Zhao YY, Hu G, Pan D, Malik AB and Hu G: YAP controls endothelial activation and vascular inflammation through TRAF6. Circ Res 123: 43-56, 2018.
77. Hutchinson JN, Ensminger AW, Clemson CM, Lynch CR, Lawrence JB and Chess A: A screen for nuclear transcripts identifies two linked noncoding RNAs associated with SC35 splicing domains. BMC Genomics 8: 39, 2007.
78. Zhang X, Hamblin MH and Yin KJ: The long noncoding RNA Malat1: Its physiological and pathophysiological functions. RNA Biol 14: 1705-1714, 2017.
79. Jin D, Guo J, Wu Y, Du J, Yang L, Wang X, Di W, Hu B, An J, Kong L, *et al*: m^{6}A mRNA methylation initiated by METTL3 directly promotes YAP translation and increases YAP activity by regulating the MALAT1-miR-1914-3p-YAP axis to induce NSCLC drug resistance and metastasis. J Hematol Oncol 12: 135, 2019.
80. Sun Y, Jiang T, Jia Y, Zou J, Wang X and Gu W: LncRNA MALAT1/miR-181a-5p affects the proliferation and adhesion of myeloma cells via regulation of Hippo-YAP signaling pathway. Cell Cycle 18: 2509-2523, 2019.
81. Wang J, Wang H, Zhang Y, Zhen N, Zhang L, Qiao Y, Weng W, Liu X, Ma L, Xiao W, *et al*: Mutual inhibition between YAP and SRSF1 maintains long non-coding RNA, Malat1-induced tumourigenesis in liver cancer. Cell Signal 26: 1048-1059, 2014.